A HUBBLE DIAGRAM OF DISTANT TYPE Ia SUPERNOVAE

MARIO HAMUY AND M. M. PHILLIPS

National Optical Astronomy Observatories,[1] Cerro Tololo Inter-American Observatory, Casilla 603, La Serena, Chile
Electronic mail: mhamuy@noao.edu,mphillips@noao.edu

JOSÉ MAZA

Departamento de Astronomía, Universidad de Chile, Casilla 36-D, Santiago, Chile
Electronic mail: jmaza@das.uchile.cl

NICHOLAS B. SUNTZEFF, R. A. SCHOMMER, AND R. AVILÉS

National Optical Astronomy Observatories, Cerro Tololo Inter-American Observatory, Casilla 603, La Serena, Chile
Electronic mail: nsuntzeff@noao.edu,rschommer@noao.edu,raviles@noao.edu

ABSTRACT

We have constructed Hubble diagrams in B and V for 13 Type Ia supernovae (SNe Ia) found in the course of the Calán/Tololo survey covering an unprecedented range in redshift ($0.01 < z < 0.1$). As opposed to other published Hubble diagrams, these are solely based on light curves obtained with CCDs, which have been carefully reduced in order to avoid background contamination. Special care was also taken in the extrapolation of peak magnitudes for the SNe that were discovered after maximum light by using five different template light curves representing the range of observed decline rates of SNe Ia. The resulting Hubble diagrams show clear evidence for a distance-dependent dispersion. Although some of the scatter could be due to the peculiar velocities of the host galaxies or to uncorrected dust absorption in the host galaxies, we argue that the dominant source is an intrinsic dispersion in the peak absolute magnitudes of SNe Ia of ~ 0.8 mag in M_B and ~ 0.5 mag in M_V. If low-luminosity events like SN 1991bg are actually a separate class of supernovae which arise from different progenitors, then the intrinsic dispersion in M_B and M_V for "normal" SNe Ia would decrease to ~ 0.3–0.5 mag. This study confirms, in general terms, the finding by Phillips [ApJ, 413, L105 (1993)] from a sample of well observed nearby SNe Ia that the absolute B and V magnitudes are correlated with the initial decline rate of the B light curve, although this effect seems to be less pronounced in the Calán/Tololo SNe. Closer inspection shows that the peak luminosity-decline rate relation is well defined over a wide range of decline rates [$0.8 < \Delta m_{15}(B) < 1.5$]; at faster decline rates the dispersion may increase, but further observations of more such events are required to verify this. Although the number of SNe studied here is relatively small, we find that galaxies having a younger stellar population appear to host the most luminous SNe Ia. This finding suggests that the progenitors of SNe Ia cover a range of masses with the most luminous events corresponding to the most massive progenitors. If ignored, this effect could introduce significant bias into determinations of both H_0 and q_0. We present Hubble diagrams in B and V for the subset of the Calán/Tololo SNe which have decline rates in the range $0.8 < \Delta m_{15}(B) < 1.5$. A dramatic decrease in the scatter in these diagrams is obtained when the data are "corrected" for the peak luminosity-decline rate relation derived from events in the Phillips sample of nearby SNe Ia covering the same range of decline rates. An analysis of published photometry for SN 1972E in NGC 5253 indicates that this supernova was a slow-declining event. Using the recently measured Cepheid distance to NGC 5253, a Hubble constant in the range $H_0 \approx 62$–67 km s^{-1} Mpc^{-1} is calculated when the peak luminosity-decline rate relation is taken into account. The result of ignoring this effect for SN 1972E is to underestimate H_0 by $\sim 15\%$.

1. INTRODUCTION

The first Hubble diagram for Type I supernovae (SNe I hereafter) was published by Kowal (1968). This study, which was carried out in the photographic band, yielded a relatively small dispersion (0.6 mag) in the maximum magnitudes of

Type I SNe, revealing the potential utility of such objects as extragalactic distance indicators. Several years later, once the existence of the Ia subclass had been recognized, the Hubble diagram was reconsidered by a number of authors (Tammann & Leibundgut 1990; Leibundgut 1990; van den Bergh & Pazder 1992; Sandage & Tammann 1993) who found a scatter in the peak magnitudes of 0.3–0.5 mag. However, a number of observational complications have hampered the determination of the intrinsic spread in the luminosities of these objects:

(1) These diagrams are nearly entirely based on nearby

TABLE 1. Colors and magnitudes of the Calán/Tololo supernovae Ia.

(1)	(2)	(3)	(4)	(5)	(6)	(7)	(8)	(9)	(10)	(11)	(12)
SN	$\log(cz)$	First Observ	B_{MAX}	V_{MAX}	$B_{MAX}-V_{MAX}$	M^B_{MAX} $+5\log(H_0/85)$	M^V_{MAX} $+5\log(H_0/85)$	$\Delta m_{15}(B)$	NaID?	Galaxy Type	$(B-V)_{GAL}$ ± 0.10
1990T	4.079(022)	+13	17.39(26)	17.27(19)	0.12(07)	-18.36(28)	-18.48(22)	1.21(10)	Weak	Sa	0.71
1990Y	4.066(022)	+14	17.88(09)	17.49(07)	0.39(02)	-17.80(15)	-18.20(13)	0.94(10)	?	?	0.56
1990af	4.176(017)	- 3	17.88(07)	17.83(05)	0.05(03)	-18.36(11)	-18.41(10)	1.56(05)	No	SB0	0.92
1991S	4.227(015)	+10	18.03(22)	17.91(14)	0.12(08)	-18.46(23)	-18.57(16)	1.11(10)	No	Sb	0.83:
1991U	3.971(028)	+11	16.32(30)	16.33(18)	-0.01(12)	-18.89(33)	-18.87(23)	1.03(10)	Weak	Sbc	0.74:
1991ag	3.621(062)	+ 4	14.72(09)	14.62(06)	0.10(02)	-18.74(32)	-18.83(32)	0.94(10)	Weak	SBb	0.46
1992J	4.124(020)	+16	17.65(59)	17.53(32)	0.12(27)	-18.32(60)	-18.44(34)	1.35(10)	No	E-S0	0.94
1992K	3.463(089)	+12	15.84(27)	15.10(11)	0.74(26)	-16.83(57)	-17.57(46)	1.88(10)	No	SBb	0.85
1992P	3.879(034)	0	16.11(07)	16.13(06)	-0.02(04)	-18.63(19)	-18.62(18)	1.17(10)	Weak	SBa	0.74
1992ae	4.351(012)	+ 4	18.54(08)	18.46(06)	0.08(05)	-18.57(10)	-18.64(08)	1.18(10)	?	?	0.65:
1992aq	4.485(009)	+ 3	19.40(08)	19.34(06)	0.06(02)	-18.37(09)	-18.43(07)	1.32(10)	?	?	1.02
1992bc	3.781(043)	-13	15.17(07)	15.24(05)	-0.07(03)	-19.08(23)	-19.01(22)	0.82(05)	No	Sab	0.67
1992bo	3.753(046)	- 7	15.86(07)	15.85(05)	0.01(03)	-18.25(24)	-18.26(24)	1.72(05)	No	E5-S0	0.97

Note: colons indicate galaxy colors uncorrected for K terms

objects ($z<0.02$). At such low redshifts the peculiar motions of individual galaxies introduce significant scatter in the velocity field associated with the Hubble flow.

(2) A quick inspection of the atlas of SNe Ia light curves (Leibundgut *et al.* 1991) reveals that most objects possess fragmentary observations. Even for SNe with frequent observations, large discrepancies (~1 mag) appear among photometry coming from different sources.

(3) Much of the data for the historical SNe Ia were obtained using photographic plates, making difficult the proper subtraction of the bright galaxy background upon which SNe are often projected. The lack of a precise definition of the photographic band introduces an additional problem when comparing observations obtained from different observers and emulsions.

(4) To derive an estimate of the peak magnitude for SNe with incomplete data, the technique of fitting an average template curve has been employed (Leibundgut *et al.* 1991). However, recent studies of well observed SNe Ia (Phillips *et al.* 1987; Phillips *et al.* 1992; Leibundgut *et al.* 1993; Maza *et al.* 1994 hereafter referred to as Paper II) have shown that the light curves displayed by these objects are not all identical. As demonstrated by Hamuy *et al.* (1993a hereafter referred to as Paper I), the error introduced by extrapolating a peak magnitude using an inappropriate template curve can be substantial.

In mid 1990, a group of staff members of the Cerro Tololo Inter-American Observatory (CTIO) and the University of Chile at Cerro Calán initiated a photographic search for supernovae with the aim of producing a moderately distant ($0.01<z<0.1$) sample suitable for cosmological studies (see Paper I). In the course of the last three years this project has led to the discovery of 50 SNe. Follow-up spectroscopic observations revealed that a significant fraction (~60%) of these objects were members of the Type Ia class. Thanks to the generous collaboration of many visiting astronomers and CTIO staff members, $BV(RI)_{KC}$ photometry has been secured with CCDs for most of these SNe, and fully reduced light curves have been produced for 13 of the SNe Ia found

between 1990 and 1992. In this paper we present the Hubble diagrams in B and V for this set of SNe, and attempt to distangle the intrinsic dispersion in the maximum magnitudes of SNe Ia from the observational errors. In Sec. 2 of this paper we present the sample of SNe used in our analysis; in Sec. 3 we show the resulting Hubble diagrams in B and V; in Sec. 4 we discuss our results; finally, in Sec. 5 we summarize our conclusions. Forthcoming papers will report on the progress of this program as further light curves become available.

2. THE SAMPLE

In this study we consider the 13 SNe Ia found in the Calán/Tololo survey whose light curves are fully reduced. These objects were found in the period 1990–92 and are listed in Table 1. The three SNe found in 1990 were already reported in Paper I. SN 1992K has been discussed separately (Hamuy *et al.* 1994, hereafter referred to as Paper III) and light curves for SNe 1992bc and 1992bo were presented in Paper II. The data for the remaining SNe will be published elsewhere. The improvement of our reduction technique[2] since the publication of Paper I led us to remeasure the photometry for SNe 1990T, 1990Y, and 1990af, and this paper makes use of these improved light curves. Table 1 contains the relevant information for the study of the Hubble diagram, presented in the following format:

Column (1): SN name.

Column (2): decimal logarithm of the observed radial velocity (cz) of the parent galaxy corrected to the Galactic

---

[2]Our original approach consisted of measuring the SN brightness with a stellar aperture and sky annulus that were kept constant in size for all epochs. Afterwards we used a deep image of the galaxy (taken once the SN had faded from sight) in order to measure the residual brightness of the galaxy at the SN position in order to correct our magnitudes. Our new technique consists of using a deep image of the SN field to subtract the light of the host galaxy from the SN frames before measuring magnitudes. This approach allows us to use a psf (point spread function) to fit the SN images. For more details about this method, the reader is referred to Paper III.

Standard of Rest, as defined by Eq. (81) in RC3 (de Vau-couleurs *et al.* 1991). The redshifts were measured from our own spectroscopic observations of the nuclei of the parent galaxies. We assigned a possible peculiar velocity compo-nent of ± 600 km s^{-1} to each galaxy, which is given in brackets in units of mdex.

Column (3): the phase (with respect to the epoch of B maximum) of the first photometric observation.

Columns (4) and (5): the apparent peak magnitudes of the SN in B and V as determined from the light curves. When the SN observations did not begin until after maximum light, we performed a χ^2 minimizing procedure with five different templates selected to represent the wide range of light curve morphologies displayed by SNe Ia (this procedure is fully explained in Papers I and III). The estimated peak magni-tudes of the SN came from the best fit obtained, and their uncertainties were derived by comparing these values with the maximum magnitudes yielded by the two next-best fits.[3] The resulting magnitudes were corrected for foreground ex-tinction in the direction of the host galaxy (Burstein & Heiles 1982), and for the K terms calculated by Hamuy *et al.* (1993b) for SNe Ia. *Note that no correction has been applied for possible obscuration in the host galaxy.* The uncertainties in the corrected magnitudes (given in brackets in units of hundreths of a magnitude) include possible errors in the adopted foreground extinction (0.06 mag in B and 0.045 in V), as well as in K terms (0.02 mag).

Column (6): the "color" of the SN, $B_{MAX} - V_{MAX}$. Note that, strictly speaking, this is not a color since B_{MAX} and V_{MAX} occur at different times. For the average template curve for SNe Ia (Leibundgut 1988), the $B - V$ color at B maximum relates to $B_{MAX} - V_{MAX}$ as follows: $(B - V)_{B(MAX)} = (B_{MAX} - V_{MAX}) - 0.02$.

Columns (7) and (8): the absolute B and V peak magni-tudes of the SN calculated from the apparent magnitudes given in columns (4) and (5), the redshift from column (2), and an assumed value of the Hubble constant of $H_0 = 85$ km s^{-1} Mpc^{-1}. The quoted error in the absolute magnitude is the result of summing in quadrature the error in the apparent magnitude, and the uncertainty in the redshift. Again, we did not include corrections for extinction in the parent galaxy.

Column (9): the parameter $\Delta m_{15}(B)$, defined by Phillips (1993) as the amount in magnitudes that the B light curve decays in the first 15 days after maximum. In cases when the SN was not discovered until after maximum, we estimated $\Delta m_{15}(B)$ from the reduced χ^2 values of the template fits. The procedure followed is illustrated in Fig. 1, where we have plotted the reduced χ^2 values for the template fits to the SNe 1990T and 1992J photometry vs the corresponding $\Delta m_{15}(B)$ parameter for each template. The value of $\Delta m_{15}(B)$ was estimated by fitting a parabola to these data. [For several of the slower-declining events, the χ^2 fits to the SN 1991bg templates did not converge to a reasonable solu-
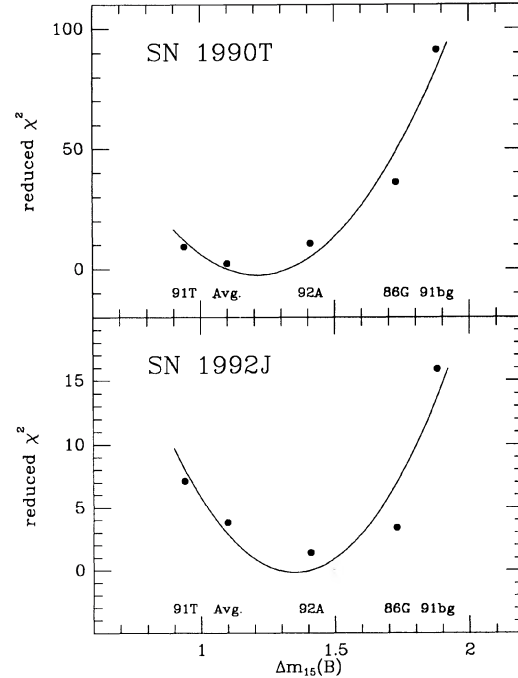

FIG. 1. The reduced χ^2 values of the five template fits to B and V photom-etry of SNe 1990T and 1992J vs the corresponding $\Delta m_{15}(B)$ parameter for each template. The curves correspond to parabolic fits to the data.

tion; in such cases the value of $\Delta m_{15}(B)$ was estimated by fitting a parabola to the reduced χ^2 values obtained from the fits to the other four templates.] This fitting procedure was followed except when the minimum χ^2 corresponded to one of the two template extremes (1991T and 1991bg); in such cases, the value of $\Delta m_{15}(B)$ was assumed to be equal to that of the template (0.94 or 1.88).[4] Applying this technique to SNe with known decline rates, we estimate an overall uncer-tainty for the interpolated $\Delta m_{15}(B)$ values of ± 0.1 mag. For those SNe observed through maximum light we estimate that the uncertainty in $\Delta m_{15}(B)$ is 0.05 mag.

Column (10): a note indicating the presence in the spec-trum of Na I D interstellar absorption due to the host galaxy. In two cases we were not able to confirm or rule out the presence of the line due to the low S/N ratio of the spectra; for one SN (1990Y) a spectrum was unavailable to us.

Column (11): the morphological type for the parent gal-axy following the classification scheme in The Hubble Atlas of Galaxies (Sandage 1961). Note that in three cases we were not able to provide a classification since the galaxies were too distant.

Column (12): the integrated $B - V$ color of the parent gal-axy corrected for foreground extinction as well as for K terms (determined from our own spectroscopic observations

---

[3] Where the magnitude differences for the next-best fits were similar, the smaller of the two differences was taken to be the uncertainty in the peak magnitude; where the magnitude differences were significantly different, the greater of the two was adopted. When the best fit corresponded to one of the template extremes (1991T or 1991bg), the error was taken to be the single magnitude difference to the next-best fit.

[4] By including SN 1991bg as one of the templates, we are implicitly assum-ing that this event represents an extension of the SN Ia phenomenon—a point which is still under some discussion (see Sec. 4). However, except for SN 1992K (shown in Paper III to be a twin of SN 1991bg), the derived $\Delta m_{15}(B)$ values do not change by more than 0.1 mag if the reduced χ^2 values for the SN 1991bg template fits are excluded.
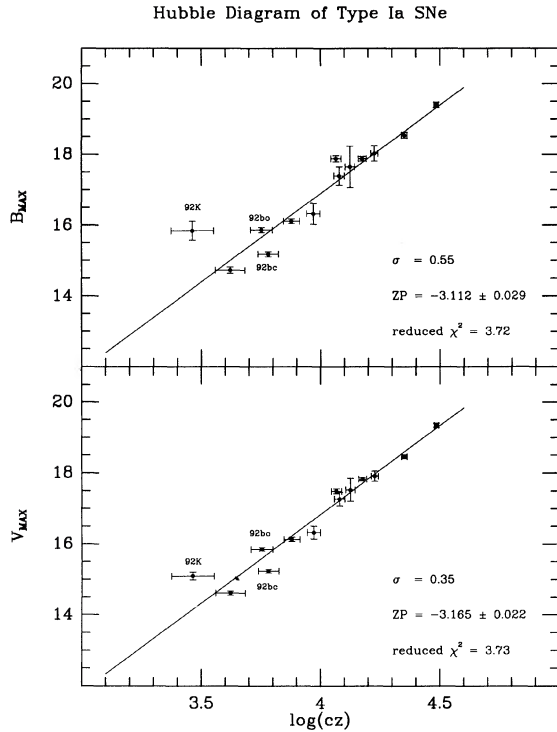
Hubble Diagram of Type Ia SNe

FIG. 2. The Hubble diagrams in B and V for the 13 Calán/Tololo SNe Ia reduced to date.

FIG. 3. The absolute B and V magnitudes of the Calán/Tololo sample of 13 SNe Ia, plotted as a function of their $B_{MAX} - V_{MAX}$ colors. The galactic reddening vectors (with slopes of 4 in B, and 3 in V) corresponding to $E(B-V)=0.2$ are indicated.

of the galaxy). For all galaxies the K correction acted to make the color bluer. In the three cases marked with a colon, the lack of an integrated spectrum prevented us from applying this correction. Thus, the quoted value must be taken with care, and only as an upper limit to the true color.

3. THE HUBBLE DIAGRAMS IN B AND V

Figure 2 shows the resulting Hubble diagrams in B and V for the Calán/Tololo SNe Ia. The ridge lines, which correspond to (weighted) least-squares fits of the data to the theoretical lines of constant luminosity, yield the following zero points and dispersions:

$$B_{MAX} = 5 \log cz - 3.112(\pm 0.029) \quad \sigma = 0.55, \qquad (1)$$

$$V_{MAX} = 5 \log cz - 3.165(\pm 0.022) \quad \sigma = 0.35. \qquad (2)$$

Note that the quoted dispersion is the simple rms deviation of the points about the fit. *The most obvious property of these diagrams is that the dispersion is greatest for the nearest SNe.* In the remainder of this section, we consider possible sources for this scatter.

3.1 Peculiar Velocities of the Host Galaxies

The fact that the deviations are greatest for the nearest objects would be expected if the scatter were due primarily to the peculiar motions of the host galaxies. This would require that several of the galaxies possess peculiar motions with respect to the pure Hubble flow considerably in excess of the value of 600 km s^{-1} assumed in the horizontal error
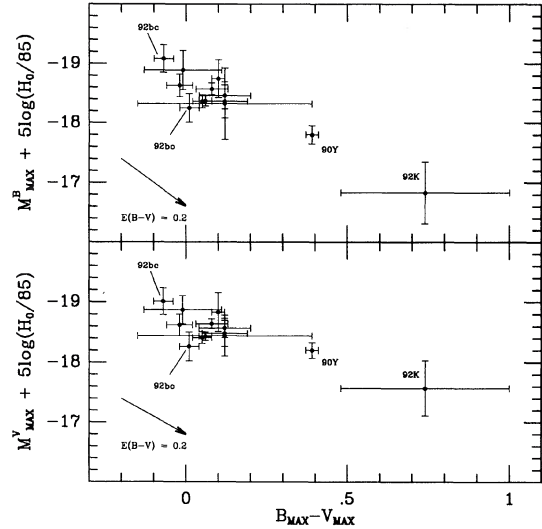
bars plotted in Fig. 2. While large scale streaming motions $\sim$1000 km s^{-1} or larger have been observed in certain directions in the sky (e.g., Dressler *et al.* 1987), we will show in Sec. *3.3* that peculiar motions are probably not the major source of the observed dispersion in the Hubble diagrams of Fig. 2.

3.2 Extinction in the Host Galaxies

Dust in the parent galaxies may also contribute to the observed dispersion in the Hubble diagrams. In order to study this possibility, we plot in Fig. 3 the absolute magnitudes of the Calán/Tololo sample of SNe as a function of the $B_{MAX} - V_{MAX}$ color. Shown for comparison in the same figure are the galactic reddening vectors (with slopes of 4 in B, and 3 in V) corresponding to a color excess of $E(B-V)$ $=0.2$. Although there is a clear trend in Fig. 3 for the less luminous SNe to be characterized by a redder color, it is almost certainly the case that dust is not the explanation for the very red color of SN 1992K. Rather, as discussed in Paper III, the spectroscopic and photometric data convincingly demonstrate that this object was a twin to the subluminous and intrinsically red SN 1991bg. Much of the spread in color for the remaining SNe in the Calán/Tololo sample could be due to dust in the host galaxies. Unfortunately, a spectrum of SN 1990Y, the second-reddest event, is not available to us, so we are unable to check on the likelihood of this explanation by searching for strong interstellar absorption lines. As noted in Table 1, the other 11 SNe showed no or weak Na I D interstellar lines, consistent with the fairly small range observed in the $B_{MAX} - V_{MAX}$ color. Thus, we conclude that most of the SNe in the Calán/Tololo sample did not suffer significant reddening due to dust in their host galaxies. This is, perhaps, not so surprising since the Calán/

Tololo search was conducted with photographic plates which generally prevent the discovery of SNe near the central parts of the galaxies (see Shaw 1979).

Of course, it is also possible that some of the spread in color observed in Fig. 3 is intrinsic. As mentioned above, this is very likely true for SN 1992K, and the work of Phillips (1993) suggests that subluminous SNe Ia may be redder in $B-V$ than brighter events. The light curves of the two best observed events in the Calán/Tololo sample, 1992bc and 1992bo, appear to support such an intrinsic spread in color, although the effect is considerably smaller than that implied by Phillips' work (see Paper II). Unfortunately, sorting out these two different possibilities—dust reddening vs an intrinsic color spread—is made difficult by the similar effects they display in a diagram like Fig. 3. It is clear, however, that great care must be exercised when assuming a single intrinsic color for all SNe Ia.

3.3. Intrinsic Dispersion in Peak Luminosity

The increased scatter in the Hubble diagrams at smaller redshifts could also be the product of a significant intrinsic dispersion in peak absolute magnitudes. Lower luminosity events would be increasingly difficult to discover at greater and greater redshifts, leading to a classical Malmquist bias. Evidence for the existence of such a spread in luminosity comes from Phillips (1993), who studied nine (nearby) well observed SNe Ia whose relative distances are known via the surface brightness fluctuations or Tully–Fisher methods. A significant (0.8 mag in B; 0.6 mag in V) intrinsic scatter in the absolute magnitudes at maximum light was found which appeared to be correlated with the initial decline rate of the B light curve [$\Delta m_{15}(B)$]. Fortunately, the Calán/Tololo sample provides an independent data set for testing the reality of such a relationship.

Figure 4 (top and central panels) shows the absolute B and V magnitudes of the 13 SNe of the Calán/Tololo sample plotted as a function of $\Delta m_{15}(B)$, on top of the least-squares fits from Phillips' sample.[5] Generally speaking, our study confirms the finding from the nearby sample in which less luminous SNe display a faster decline rate in their B light curves—hence, most or all of the observed scatter in the Hubble diagrams of Fig. 2 is likely intrinsic. Nevertheless, three of the events in the Calán/Tololo sample—SNe 1990Y, 1990af, and 1992bo—deviate significantly from the fits to the nearby sample. In the case of SN 1990Y, the difference may well be due to uncorrected dust absorption in the host galaxy (see Sec. 3.2 and below), but this cannot be the explanation for the other two events which are more luminous than the Phillips relations would predict. This pair of objects, which are among the best-observed of the Calán/Tololo SNe, suggests a weaker dependence of the absolute luminosities upon the decline rate (see also Paper II) over the

---

[5]The value of H_0 used in this paper to calculate the absolute magnitudes of the Calán/Tololo sample was selected to correspond to the Hubble constant yielded by the surface brightness fluctuations and the Tully–Fisher methods (Jacoby *et al.* 1992). This choice was made with the aim of tying the absolute magnitudes to the same scale used by Phillips, and does not reflect a preference on our part for a particular value of H_0.
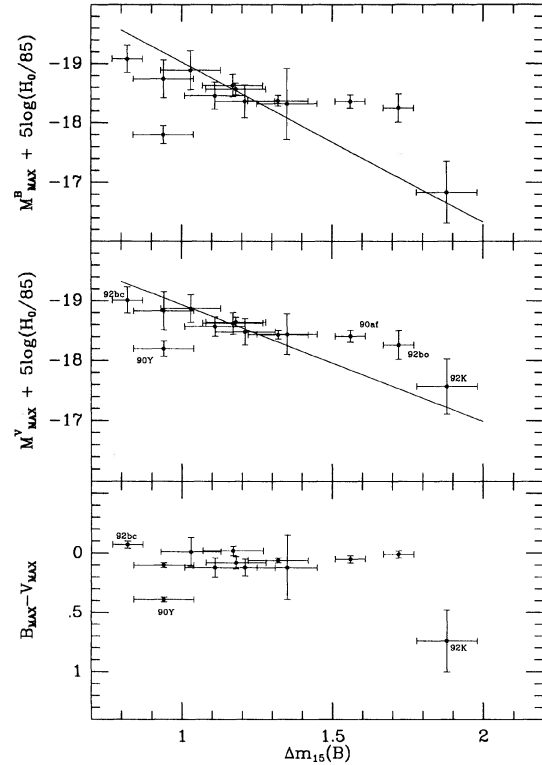

FIG. 4. The absolute B and V magnitudes of the 13 Calán/Tololo SNe Ia plotted as a function of $\Delta m_{15}(B)$ [the initial decline rate of the B light curve as defined by Phillips (1993)]. For comparison, we have overplotted as ridge lines the fits obtained by Phillips (1993) to his set of nearby SNe Ia (top and central panels). Also shown is the $B_{MAX}-V_{MAX}$ color of the Calán/Tololo sample of SNe Ia, plotted as a function of $\Delta m_{15}(B)$ (bottom panel).

range $0.82 \leq \Delta m_{15}(B) \leq 1.72$ mag. The linear relationship observed over this range of decline rates in the Calán/Tololo sample is followed then by the sudden drop in luminosity of SN 1992K at $\Delta m_{15}(B)=1.88$, suggesting either that the relationship becomes nonlinear for such fast declining events or that there is a greater intrinsic spread in luminosity at decline rates $\Delta m_{15}(B)>1.5$.

To examine the latter point in more detail, we have replotted in Fig. 5 the same diagram, but this time replacing the fit to the Phillips' (1993) sample with the points for the individual SNe. From this figure it is evident that, excluding SN 1990Y (because of our suspicion of reddening), the relationship between peak absolute magnitude and initial decline rate is actually quite well defined for the "slow" events, i.e., those with $\Delta m_{15}(B)<1.5$ mag. However, at faster decline rates, the dispersion appears to increase, especially in the B band. SN 1991bg and its twin, SN 1992K, clearly do not lie on the extension of the peak magnitude–decline rate relation observed for the "slow" events, but this is perhaps not surprising since both SNe were spectroscopically distinct from typical SNe Ia. More difficult to understand is the case of SN 1971I, which is apparently more than a magnitude fainter in B than the Calán/Tololo SNe with similar decline rates, 1990af and 1992bo. However, the published photometry for SN 1971I is less precise than that for any of the other SNe plotted in Fig. 5 and, although SN 1971I was located far
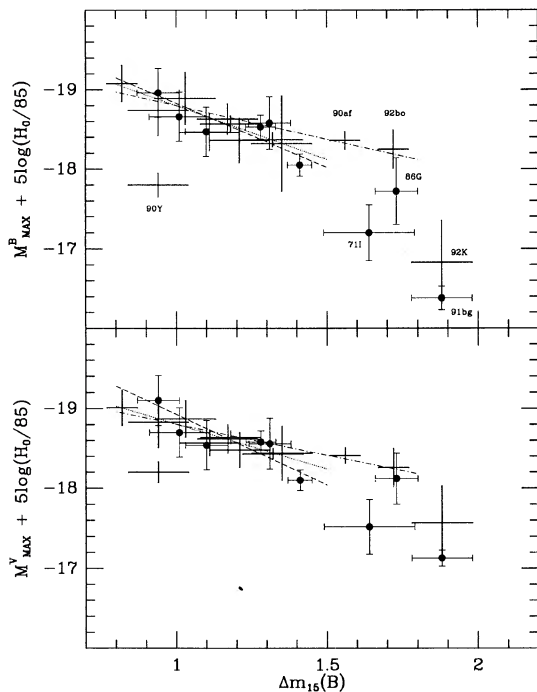
FIG. 5. The absolute B and V magnitudes of the 13 Calán/Tololo SNe Ia plotted as a function of $\Delta m_{15}(B)$. For comparison, the absolute B and V magnitudes of the nine well observed SNe Ia from Phillips (1993) sample are plotted as solid dots. Linear regression fits to the six events in the Phillips sample with $0.8 < \Delta m_{15}(B) < 1.5$ are shown as dashed lines; fits to the nine Calán/Tololo SNe Ia (excluding SN 1990Y due to suspicions of dust reddening) with initial decline rates in the same range are plotted as dotted lines. Fits to the 11 Calán/Tololo SNe Ia which meet the alternative selection criterion of $-0.25 < B_{MAX} - V_{MAX} < +0.25$ suggested by Vaughan *et al.* (1994) are shown as dot-dashed lines.
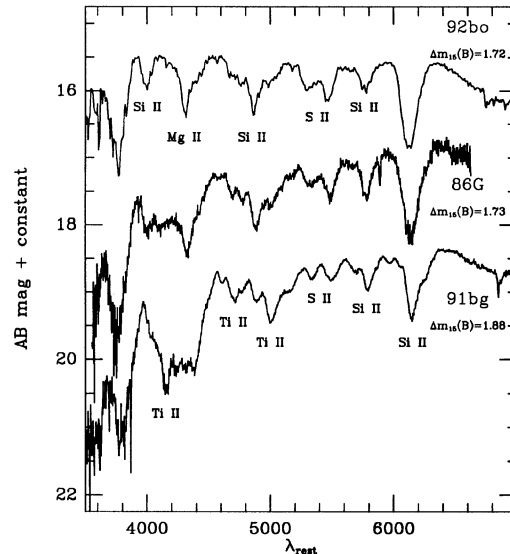
FIG. 6. Comparison of the maximum light spectra of the fast-declining SNe 1992bo, 1986G, and 1991bg. Note the subtle spectroscopic differences in the region of the Ti II absorption between SNe 1992bo and 1986G in spite of the identical initial decline rates of the B light curves.

from the nucleus and spiral arms, dust absorption in the host galaxy, NGC 5055, cannot be completely ruled out. The other object in Phillips' sample which lies in this part of the diagram is SN 1986G. Unfortunately, SN 1986G was significantly reddened by the prominent dust lane in its host galaxy, NGC 5128, and so we can only guess at its intrinsic brightness. The magnitudes plotted in Fig. 5 were derived by Phillips (1993) assuming an intrinsic $B_{MAX} - V_{MAX}$ color of 0.40, which is similar to the (rather uncertain) color observed for SN 1971I. If we, instead, assume that SN 1986G had an intrinsic color of $B_{MAX} - V_{MAX} = 0.01$ like SN 1992bo, absolute magnitudes of $M_B \approx M_V \approx -19.2 \pm 0.3$ are implied which would make 1986G the most luminous SN plotted in Fig. 5. To force SN 1986G to be equal in luminosity to SN 1992bo in both B and V would require a rather low value of $R = A_V / E(B-V) = 2.0$ for the dust in NGC 5128; in fact, this is only slightly smaller than the value of $R = 2.40 \pm 0.13$ deduced by Hough *et al.* (1987) from polarization observations of 1986G. Nevertheless, as shown in Fig. 6, the spectra of SNe 1986G and 1992bo displayed subtle differences at maximum light. Included in Fig. 6 is the spectrum of the extreme fast-declining SN 1991bg, also obtained near maximum light. The most obvious spectroscopic peculiarity of SN 1991bg was the presence of strong Ti II absorption, especially in the 4000–4400 Å region (Filippenko *et al.* 1992).

Note that the spectrum of SN 1986G also shows clear evidence of Ti II absorption, while that of 1992bo does not. Since this absorption affects the B band, the intrinsic $B_{MAX} - V_{MAX}$ color of 1986G could well have been somewhat redder than that of 1992bo. Unfortunately, the published spectroscopic data for SN 1971I are of insufficient quality to judge the presence or absence of the Ti II feature.

In the bottom panel of Fig. 4 we have plotted the $B_{MAX} - V_{MAX}$ color as a function of $\Delta m_{15}(B)$ for the Calán/Tololo SNe. We note that the slowest-declining event in the sample, SN 1992bc, had the bluest $B_{MAX} - V_{MAX}$ color, while the fastest decliner, 1992K, was the reddest. Nevertheless, over the range $0.82 \leq \Delta m_{15}(B) \leq 1.72$, there is little evidence for a strong dependence of $B_{MAX} - V_{MAX}$ on the initial decline rate. The exceptional events in this diagram are clearly SN 1992K, which Hamuy *et al.* (1994) have argued was intrinsically red and subluminous, and SN 1990Y which appears too red ($B_{MAX} - V_{MAX} = 0.39$) given its low decline rate. If we assume that the red color of SN 1990Y was the product of dust absorption in its host galaxy and correct the photometry using a normal reddening law for an intrinsic color $B_{MAX} - V_{MAX} = 0.05$ similar to the other SNe in the Calán/Tololo sample with a similar decline rate, absolute magnitudes of $M_B^0 \approx M_V^0 \approx -19.2(\pm 0.2) + 5 \log(H_0/85)$ are implied, which are consistent with the peak brightness–decline rate relation seen in Figs. 4 and 5. However, lacking a spectrum of SN 1990Y in which we would expect to see moderately strong interstellar absorption features, we cannot unequivocally rule out the possibility that this event was intrinsically red and subluminous.

Figure 7 shows the B and V absolute magnitudes of the 13 SNe of the Calán/Tololo sample (open circles) plotted as a function of the morphological type of the parent galaxies. For this purpose we have separated the morphological types
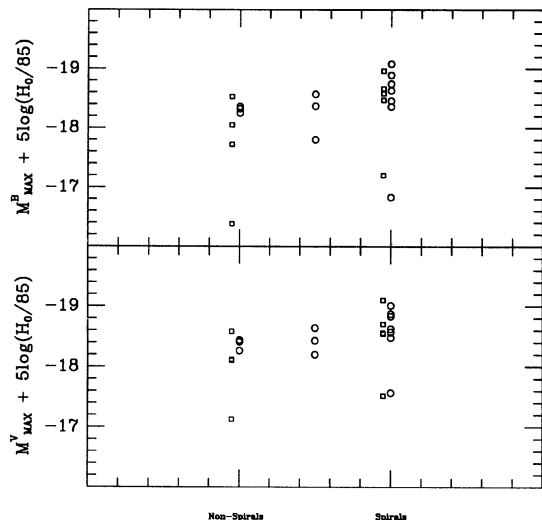
FIG. 7. The absolute B and V magnitudes of the Calán/Tololo SNe Ia (open circles) and the well observed events studied by Phillips (1993) (open squares) plotted as a function of the morphological types of their host galaxies. The host galaxies of the three SNe plotted in between the two basic categories (spirals and non-spirals) could not be properly classified due to their distances.

FIG. 8. The absolute B and V magnitudes of the Calán/Tololo SNe Ia plotted as a function of the integrated $B - V$ colors of their host galaxies.

into two basic categories, namely, spirals and nonspirals. The three SNe for which we were not able to provide an adequate classification are plotted between the two classes. Due to the small number of objects of the distant sample, we have also added in Fig. 7 the nine SNe from Phillips' sample (open squares). Although the total number of galaxies in these samples is still relatively small, we are struck by the fact that the most luminous SNe were hosted by spiral galaxies.[6] Note that this dependence on galaxy type is not the result of uncorrected dust absorption, which would be expected to make SNe in spiral galaxies less luminous on average.

An alternative way to explore the relationship between SNe Ia and their environments is to look at the integrated colors of the parent galaxies. Ideally, one would like to have an estimate of the color of the galaxy right at the position of the SN, but this is impossible for events lying far from the nucleus of their parent galaxy. Figure 8 shows the B and V absolute magnitudes of the 13 SNe of the Calán/Tololo sample versus the integrated color of the host galaxies. In general, we see that the brightest SNe appeared in the bluest galaxies, which are presumably those with the most active star formation. The main exception to this trend is SN 1990Y, but, as discussed above, dust absorption would explain the low luminosity of this event.

---

[6]A similar conclusion was reached by van den Bergh & Pazder (1992) under the assumption of an intrinsic $B - V$ color at maximum of -0.25. However, Figs. 3 and 4 (bottom panel) show that the typical intrinsic color of SNe Ia is ~ 0.0, in which case the effect found by van den Bergh & Pazder disappears. A number of years ago, Pskovskii (1967) also found that SNe Ia in spirals and irregular galaxies were more luminous than those in ellipticals and S0's, but this result depended strongly on dust absorption corrections made for the SNe Ia in spirals.
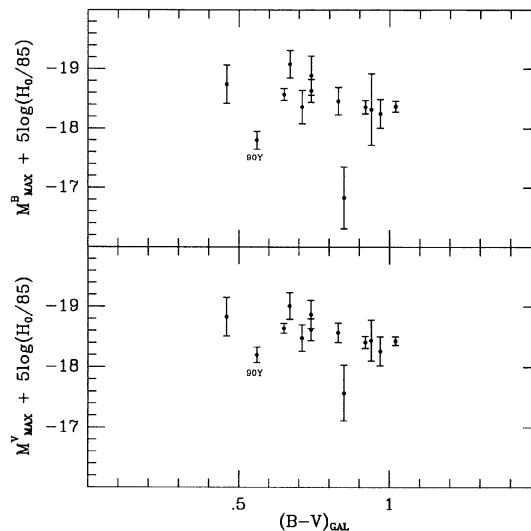
4. DISCUSSION

The data for the 13 Calán/Tololo SNe Ia presented in the previous section confirm, in general terms, the peak luminosity–decline rate relationship found by Phillips (1993). If we assume that the faintest SNe Ia have $M_B \sim -17.0 + 5 \log(H_0/85)$, then the Calán/Tololo search, which is characterized by a limiting magnitude of $m_{pg} \sim 19$, will start to become significantly incomplete at $z > 0.035$ [$\log(cz) > 4.02$] (see Paper III). For the six SNe in the Calán/Tololo sample with redshifts less than this value, the observed dispersion is 0.78 mag in M_B and 0.50 mag in M_V. These are very similar to the dispersions of 0.79 mag in M_B and 0.59 mag in M_V found by Phillips (1993) for his nearby sample of nine well observed events, suggesting that such values are, indeed, representative of a volume-limited sample of SNe Ia. *Hence, we conclude that the distance-dependent dispersion observed in the SNe Ia Hubble diagrams plotted in Fig. 2 is largely due to an intrinsic spread in the peak luminosities of these events.* Leaving aside for the moment questions of the suitability of SNe Ia as cosmological standard candles, this conclusion has important and obvious implications for the current debate over the nature of the progenitors of SNe Ia and the explosion mechanism(s) (e.g., see Woosley & Weaver 1994, and references therein).

Relevant to this discussion is the question of whether SNe like 1991bg and 1992K should be counted as legitimate type Ia events. Filippenko *et al.* (1992) and Leibundgut *et al.* (1993) argued that SN 1991bg, while clearly an extreme case, could still be understood in the general context of an exploding white dwarf, and subsequent attempts to model this object as the explosion of a sub-Chandrasekhar mass white dwarf (Ruiz-Lapuente *et al.* 1993; Woosley & Weaver 1994) have met with reasonable success. Recently, however, Woosley *et al.* (1994) have speculated that events such as 1991bg and 1992K could be explained, instead, as the explosion of a helium star that has experienced significant mass
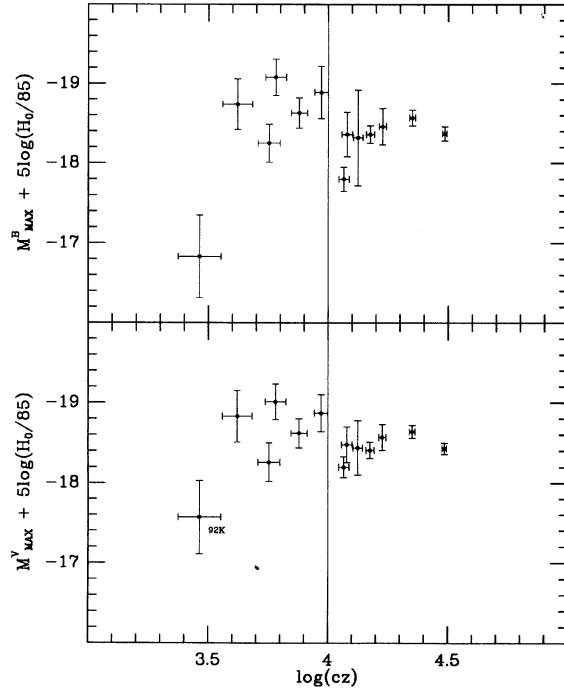
FIG. 9. The absolute B and V magnitudes of the Calán/Tololo SNe Ia plotted as a function of redshift. The vertical line at $\log cz = 4$ (10 000 km s^{-1}) illustrates the separation of the sample into two groups. The seven more distant SNe yield $\langle M_B \rangle = -18.32(\pm 0.24) + 5 \log(H_0/85)$ and $\langle M_V \rangle = -18.45(\pm 0.14) + 5 \log(H_0/85)$, whereas the six nearer ones yield $\langle M_B \rangle = -18.40(\pm 0.82) + 5 \log(H_0/85)$ and $\langle M_V \rangle = -18.53(\pm 0.54) + 5 \log(H_0/85)$. The SN responsible for the large scatter in the nearby bin is SN 1992K; excluding this object increases $\langle M_B \rangle$ to $-18.72(\pm 0.31) + 5 \log(H_0/85)$ and $\langle M_V \rangle$ to $-18.72(\pm 0.29) + 5 \log(H_0/85)$.

loss. If SN 1992K is excluded from the Calán/Tololo sample of SNe with $z < 0.035$, the dispersions in peak absolute magnitude decrease to 0.28 mag in M_B and 0.27 mag in M_V; excluding SN 1991bg from Phillips' (1993) nearby sample yields dispersions of 0.58 mag in M_B and 0.49 mag in M_V. Hence, if the progenitors of 1991bg-like events are helium stars, then the intrinsic dispersion in M_B and M_V for SNe Ia with (presumably) white dwarfs is most likely of order 0.3–0.5 mag. It should be emphasized, however, that the host galaxy of SN 1991bg was an elliptical galaxy and, therefore, an unlikely place to find a helium star.

An intriguing feature of the Hubble diagrams of Fig. 2 is the fact that the nearby SNe appear to be brighter on average compared to the more distant ones. Figure 9 shows the absolute magnitudes in B and V plotted as a function of redshift. Separating the sample into two groups at a redshift of $\log cz = 4$ (10 000 km s^{-1}), we get $\langle M_B \rangle = -18.32(\pm 0.24) + 5 \log(H_0/85)$ for the seven more distant SNe and $\langle M_B \rangle = -18.40(\pm 0.82) + 5 \log(H_0/85)$ for the six nearer ones. The SN responsible for the large scatter in the nearby bin is SN 1992K; excluding this object increases $\langle M_B \rangle$ to $-18.72(\pm 0.31) + 5 \log(H_0/85)$. Some insight into the origin of this apparent difference, which is actually the opposite of that which would be expected for a normal Malmquist bias, is provided by Fig. 10, where we have plotted the morphological types of the parent galaxies as a function of redshift.
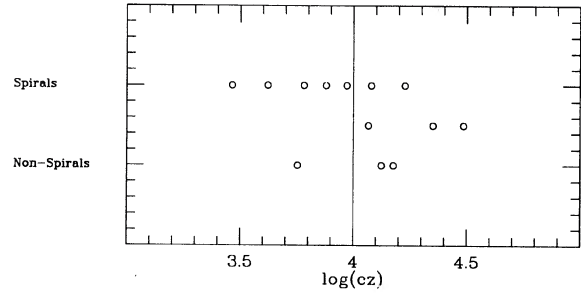

FIG. 10. The morphological types of the host galaxies of the Calán/Tololo SNe Ia plotted as a function of redshift. Note that the ratio of spirals/nonspirals is significantly higher in the nearby sample ($\log cz < 4$) than in the more distant group ($\log cz > 4$).

Note that five of the six SNe with $\log cz < 4$ occurred in spiral galaxies, consistent with the fact that these events are considerably more common in spirals than in E/S0 galaxies (e.g., Capellaro *et al.* 1993). However, Fig. 10 shows that the fraction of SNe discovered in spirals for the subsample with $\log cz > 4$ appears to be significantly smaller. Taking into account our previous finding that SNe Ia in spirals are brighter on average than those occurring in nonspirals (see Fig. 7), it is thus not surprising that the nearby group of SNe contains more of the intrinsically most-luminous events. Left unanswered, however, is the question of why the ratio of spirals to nonspirals is so different for the nearby and most distant samples? Several possible explanations occur to us:

(1) *Small number statistics.* The number of SNe in our sample is sufficiently small that it is possible that much of the observed luminosity difference between the SNe with $\log cz < 4$ and the most distant events is due to chance. Indeed, even if SN 1992K is deleted from the nearby events, the difference in mean absolute magnitudes between the two subsamples is only significant at roughly the $1–2\sigma$ level.

(2) *Radial effects.* It is possible that the intrinsically brightest SNe occur preferentially at smaller galactic radii (e.g., if SN Ia luminosities were proportional to the metallicity of the surrounding stellar population). Since, in a photographic search, the more distant SNe will tend to be discovered at larger galactic radii (Shaw 1979), this could lead to an effect similar to that observed.

(3) *Spiral arms.* The fact that the disks of spiral galaxies are much less smooth and regular than the surface brightness profiles of E and S0 galaxies could cause the discovery rate of SNe in spirals to cutoff more rapidly as a function of redshift. This would cause the ratio of SNe in spirals to those in nonspirals to decrease between nearby and distant samples, thus leading to a difference in average luminosity.

With the current sample of only 13 events, it is impossible to tell which (if any) of these hypotheses are correct. We plan to return to this question once we have completed the data reduction for the complete sample of Calán/Tololo SNe Ia (~ 25–30 events).

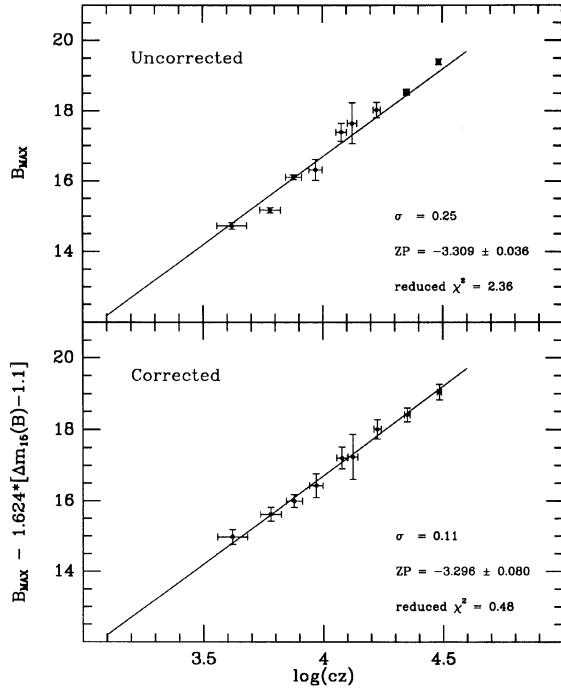Although the existence of a peak luminosity–decline rate

FIG. 11. (top panel) The Hubble diagram in B for the SNe Ia in the Calán/Tololo sample with initial decline rates in the range $0.8 \leq \Delta m_{15}(B) \leq 1.5$. The suspected obscured SN 1990Y has also been excluded. (bottom panel) The Hubble diagram for the same nine events after correction for the peak luminosity–decline rate dependence.
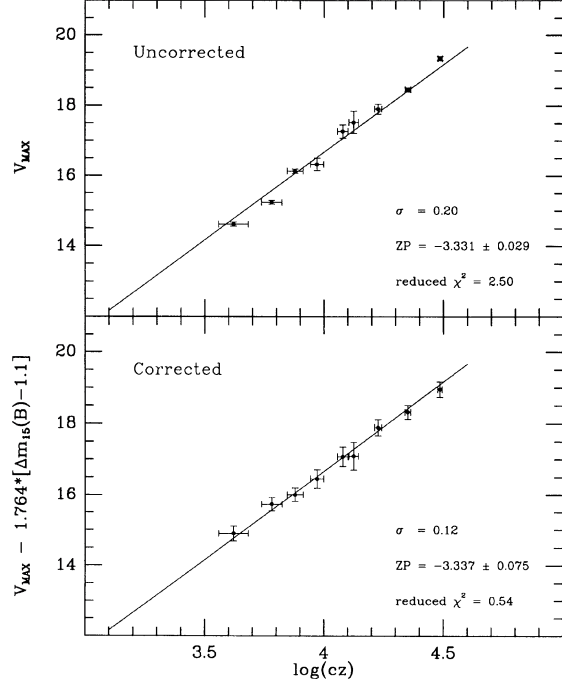

FIG. 12. (top panel) The Hubble diagram in V for the SNe Ia in the Calán/Tololo sample with initial decline rates in the range $0.8 \leq \Delta m_{15}(B) \leq 1.5$. The suspected obscured SN 1990Y has also been excluded. (bottom panel) The Hubble diagram for the same nine events after correction for the peak luminosity–decline rate dependence.

relation clearly complicates the usage of SNe Ia as cosmological standard candles, it should, in principle, be possible to correct the observed Hubble diagram for this effect, as long as we limit consideration to events with precise, well sampled light curves. We have shown that the peak luminosity–decline rate relation is tightly defined over the range of initial decline rates $0.8 < \Delta m_{15}(B) < 1.5$, but that at faster decline rates the dispersion may increase significantly. In the upper halves of Figs. 11 and 12, we show the Hubble diagrams for the Calán/Tololo SNe with $0.8 < \Delta m_{15}(B) < 1.5$. Note that SN 1990Y is not plotted due to our suspicion that it is significantly reddened by dust. Linear regression fits to the data for this subsample give the following zero points and rms dispersions:

$$B_{\mathrm{MAX}} = 5 \log cz - 3.309(\pm 0.036) \quad \sigma = 0.25, \qquad (3)$$

$$V_{\mathrm{MAX}} = 5 \log cz - 3.331(\pm 0.029) \quad \sigma = 0.20. \qquad (4)$$

The rms dispersion for this subsample is already considerably less than that obtained for the full sample of 13 events [cf. Eqs. (1) and (2)], consistent with the suggestion by Saha *et al.* (1994b) that the rejection of events with $\Delta m_{15}(B) > 1.5$ will produce samples of SNe Ia which closely resemble the traditional prototypes such as 1937C and 1981B. Nevertheless, an even more dramatic decrease in the dispersion is obtained by correcting for the peak luminosity–decline rate relation. Fits to the peak luminosity–decline rate [M vs $\Delta m_{15}(B)$] relation in B and V for the six events with $\Delta m_{15}(B) < 1.5$ in the Phillips (1993) sample of nearby SNe

Ia are plotted as dashed lines in Fig. 5. The observed magnitudes of the Calán/Tololo subsample "corrected" for the slopes of these fits (1.624 ± 0.582 in B, 1.764 ± 0.570 in V) are plotted in the bottom halves of Figs. 11 and 12 along with the following linear regression fits:

$$B_{\mathrm{MAX}} - 1.624[\Delta m_{15}(B) - 1.1]$$
$$= 5 \log cz - 3.296(\pm 0.080) \quad \sigma = 0.11, \qquad (5)$$

$$V_{\mathrm{MAX}} - 1.764[\Delta m_{15}(B) - 1.1]$$
$$= 5 \log cz - 3.337(\pm 0.075) \quad \sigma = 0.12. \qquad (6)$$

The second term on the left of these equations corrects the observed magnitudes of each SN to the equivalent magnitudes of an event with $\Delta m_{15}(B) = 1.1$ mag. The dispersions for these "corrected" Hubble diagrams are spectacularly small; indeed, they are now consistent with being entirely due to observational error (the reduced χ^2 is 0.48 for B and 0.54 for V). *It is crucial to note that this improvement in the scatter for the distant SNe Ia was obtained by application of the peak luminosity decline relation inferred from a completely independent sample of nearby events.*

As further SNe Ia with well observed light curves become available, it should be possible to obtain more precise estimates for the slopes of the peak luminosity–decline rate relation. Indeed, we can use the Calán/Tololo SNe alone to solve simultaneously for the zero point of the Hubble relation and the slope of the peak absolute magnitude–decline rate relation. This approach has the advantage that the rela-

tive distances of the Calán/Tololo sample are likely to be more reliable because they are based purely on the Hubble flow. On the other hand, possible magnitude-dependent selection effects in the Calán/Tololo sample could bias the slope of the peak luminosity–decline rate relation. Bearing in mind these advantages and disadvantages, for the same subsample of nine events with $0.8 < \Delta m_{15}(B) < 1.5$ (again excluding SN 1990Y), we obtain the following fits:

$$B_{MAX} - 1.365(\pm 0.275)[\Delta m_{15}(B) - 1.1]$$
$$= 5 \log cz - 3.311(\pm 0.052) \quad \sigma = 0.11, \qquad (7)$$

$$V_{MAX} - 1.142(\pm 0.240)[\Delta m_{15}(B) - 1.1]$$
$$= 5 \log cz - 3.339(\pm 0.046) \quad \sigma = 0.06. \qquad (8)$$

These slopes for the peak luminosity–decline rate relation (plotted in Fig. 5 as dotted lines) are somewhat smaller than the values obtained above for the Phillips (1993) sample, but still consistent within the errors of both estimates.

The preceding discussion suggests that, in spite of the significant intrinsic spread in peak absolute magnitude observed for SNe Ia, the subset of these objects with initial decline rates in the range $0.8 < \Delta m_{15}(B) < 1.5$ can be used as effective standard candles after correction for the peak luminosity–decline rate relation. In a recent paper, Vaughan *et al.* (1994) have proposed two alternative criteria for obtaining "objective" subsamples of SNe Ia: (1) the application of a luminosity cutoff at $M_B = M_V = -18.0 + 5 \log(H_0/85)$, or (2) the combination of a color restriction $(-0.25 < B_{MAX} - V_{MAX} < +0.25)$ and the requirement of no obvious spectroscopic "peculiarity." While the application of a luminosity cutoff may be acceptable for defining samples of relatively nearby SNe Ia to be used for measuring H_0, it is clearly problematic for determining q_0 since a cosmological model must be assumed to calculate the absolute magnitudes. The alternative of requiring $-0.25 < B_{MAX} - V_{MAX} < +0.25$ and "no obvious spectroscopic peculiarity" would appear less objective, although to judge "spectroscopic peculiarity" requires obtaining reasonably high signal-to-noise spectra within a few days of maximum light. We therefore consider the consequences of application of the color criterion alone to the Calán/Tololo sample. A check of Table 1 shows that only two events—SNe 1990Y and 1992K—have $B_{MAX} - V_{MAX}$ colors that fall outside the above range. Linear regression fits to the remaining 11 SNe Ia which ignore the peak luminosity–decline rate relation give the following zero points and rms dispersions:

$$B_{MAX} = 5 \log cz - 3.202(\pm 0.030) \quad \sigma = 0.25, \qquad (9)$$

$$V_{MAX} = 5 \log cz - 3.225(\pm 0.024) \quad \sigma = 0.22. \qquad (10)$$

Alternative fits which solve simultaneously for the zero point of the Hubble relation and the slope of the peak absolute magnitude–decline rate relation are as follows:

$$B_{MAX} - 0.847(\pm 0.128)[\Delta m_{15}(B) - 1.1]$$
$$= 5 \log cz - 3.359(\pm 0.047) \quad \sigma = 0.15, \qquad (11)$$

$$V_{MAX} - 0.787(\pm 0.109)[\Delta m_{15}(B) - 1.1]$$
$$= 5 \log cz - 3.375(\pm 0.040) \quad \sigma = 0.09. \qquad (12)$$

These slopes for the peak luminosity–decline rate, which are illustrated in Fig. 5 by the dot-dashed lines, are significantly less steep than those obtained using the decline rate as the selection criterion due to the inclusion in the subsample of SNe 1990af and 1992bo. Whether they are correct or not depends on whether there is a significant dispersion in peak luminosity for SNe Ia with decline rates in the range $1.5 < \Delta m_{15}(B) < 1.8$ (see discussion in Sec. *3.3*). In any case, the three fits shown in Fig. 5 illustrate quite well the current range of uncertainty in the exact form of the dependence of the peak absolute magnitude on the initial decline rate; further improvement will require precise light curves for larger samples of SNe Ia.

Sandage and collaborators have recently measured Cepheid distances to the host galaxies of three nearby SNe Ia (SN 1937C in IC 4182 and SNe 1895B and 1972E in NGC 5253), and have used these events to calibrate the Hubble diagram of these objects (Sandage *et al.* 1992, 1994; Saha *et al.* 1994a, b). The resulting mean Hubble constants determined by these authors are

$$H_0(B) = 50 \pm 8 \quad \text{km s}^{-1} \text{Mpc}^{-1},$$

and

$$H_0(V) = 54 \pm 8 \quad \text{km s}^{-1} \text{Mpc}^{-1}$$

(Saha *et al.* 1994b). Since these values were calculated without including corrections for the peak luminosity–decline rate relation, a reexamination of the Hubble constant based on the Hubble relations derived from the Calán/Tololo SNe would seem in order.

We consider first SN 1972E in NGC 5253.[7] Although this object was not discovered until after maximum light, extensive photoelectric photometry was obtained by several groups at different sites (see Phillips & Eggen 1994, and references therein). Figure 13 shows our attempts to fit the B and V light curves of SN 1972E to the five templates which we use to represent the range of observed decline rates. As is seen visually, and also in the plot in Fig. 14 of the reduced χ^2 values vs the decline rates of the templates, it is clear that 1972E was a slow declining event. (Indeed, the χ^2 minimizing procedure did not converge to a sensible solution using the SN 1991bg templates.) Since the minimum of the reduced χ^2 values corresponds to the fit to the SN 1991T template, we shall assume a decline rate of $\Delta m_{15}(B) = 0.94 \pm 0.10$ mag for SN 1972E; likewise, from this same fit we estimate the maximum light magnitudes to be

$$B_{MAX} = 8.61 \pm 0.21,$$

and

$$V_{MAX} = 8.61 \pm 0.12.$$

---

[7]SN 1895B was also observed in NGC 5253, but the available photometry of this event is of such poor quality (see Leibundgut *et al.* 1991) that we shall not consider it in the present discussion.
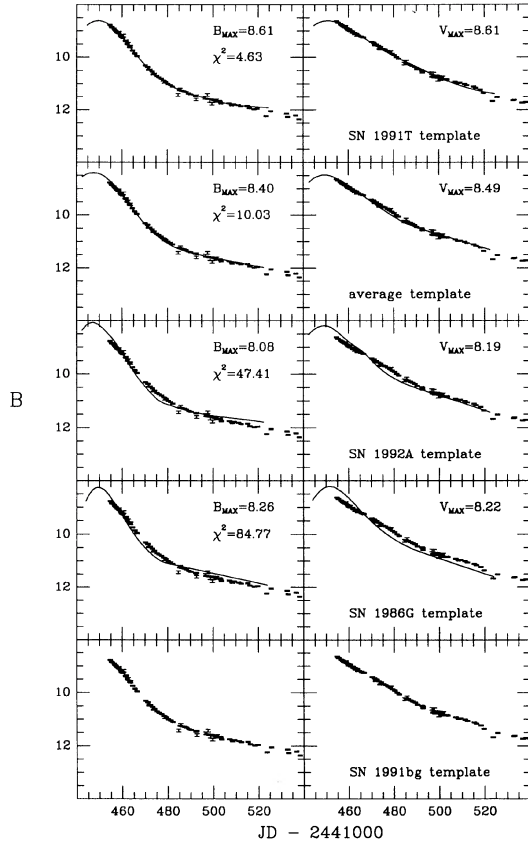
FIG. 13. Fits of the B and V photometry of SN 1972E to five template light curves selected to represent the full range of post-maximum decline rates observed for SNe Ia. Note that fits to the SN 1991bg template are not shown since the χ^2 minimizing procedure did not converge to a reasonable initial solution.

These magnitudes are very similar to the ones assumed by Saha *et al.* (1994b), but our error bars are larger. We feel that our error estimates, which were obtained by comparing the peak magnitudes yielded by the SN 1991T and average templates, are more realistic. To convert these values to absolute magnitudes, we assume the apparent Cepheid distance
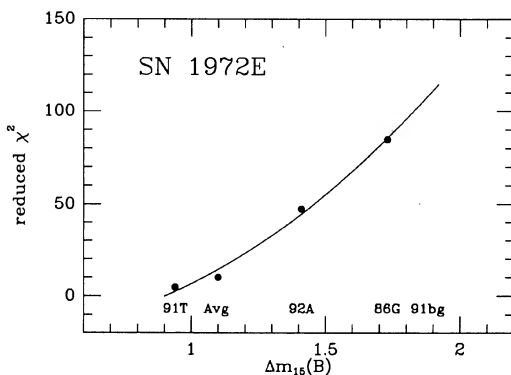

FIG. 14. The reduced χ^2 values of the four template fits to the B and V photometry of SN 1972E plotted vs the corresponding $\Delta m_{15}(B)$ parameter for each template. The curve corresponds to a parabolic fit to the data.

modulus of $(m-M)_{A_V}=28.10\pm0.10$ derived by Saha *et al.* (1994b). For the galactic reddening, we adopt a value of $E(B-V)=0.05\pm0.02$ mag (Burstein & Heiles 1982) and, following Saha *et al.* (1994b), we assume that the differential reddening between the Cepheids and SN 1972E was $E(B-V)=0.00\pm0.05$ mag. Taking into account the error in the zero point of the Cepheid calibration (assumed to be ±0.15 mag) then gives

$$M^B_{\text{MAX}}=-19.54\pm0.34,$$

and

$$M^V_{\text{MAX}}=-19.49\pm0.26.$$

From the "uncorrected" Hubble relations [Eqs. (3) and (4)] obtained for the subsample of nine Calán/Tololo SNe Ia which meet the decline rate criterion of $0.8<\Delta m_{15}(B)<1.5$, we have

$$\log H_0=0.2[M^B_{\text{MAX}}+28.309(\pm0.036)], \qquad (13)$$

and

$$\log H_0=0.2[M^V_{\text{MAX}}+28.331(\pm0.029)]. \qquad (14)$$

Taking into account the uncertainty introduced by the observed scatter of the individual SNe in the Hubble diagram (0.25 in B, and 0.20 in V), we therefore obtain

$$H_0(B)=57\pm11$$

and

$$H_0(V)=59\pm9.$$

The difference between these values and those quoted by Saha *et al.* (1994b) is due mostly to the small difference in zero points for the assumed Hubble laws; the larger error bars attached to our estimates reflect the fact that we have taken into account the uncertainties in the zero point of the Cepheid calibration, as well as larger errors for the apparent magnitudes of SN 1972E.

If we now repeat these calculations taking into account the peak luminosity–decline rate relation [Eqs. (5) and (6)] as estimated from the Phillips (1993) sample of nearby SNe Ia, we have

$$\log H_0=0.2\{M^B_{\text{MAX}}-1.624(\pm0.582)[\Delta m_{15}(B)-1.1]$$
$$+28.296(\pm0.080)\}, \qquad (15)$$

and

$$\log H_0=0.2\{M^V_{\text{MAX}}-1.764(\pm0.570)[\Delta m_{15}(B)-1.1]$$
$$+28.337(\pm0.075)\}. \qquad (16)$$

For SN 1972E the correction to the absolute magnitudes is given by the difference between its decline rate $\Delta m_{15}(B)=0.94\pm0.10$ and $\Delta m_{15}(B)=1.1$. Taking into account again the uncertainty introduced by the observed scatter of the individual SNe in the "corrected" Hubble diagrams (0.11 mag in B, and 0.12 mag in V), we obtain

$$H_0(B)=64\pm12,$$

and

$$H_0(V)=67\pm11.$$

Repeating this calculation using the fits given in Eqs. (7) and (8) for the subsample of Calán/Tololo SNe Ia which meet the decline rate selection criterion yields

$$H_0(B) = 63 \pm 11,$$

and

$$H_0(V) = 64 \pm 9.$$

Application of the fits [Eqs. (11) and (12)] to the Calán/Tololo sample resulting from the Vaughan *et al.* (1994) color criterion gives

$$H_0(B) = 62 \pm 11,$$

and

$$H_0(V) = 63 \pm 8,$$

which are to be compared with the values of

$$H_0(B) = 54 \pm 11,$$

and

$$H_0(V) = 56 \pm 9$$

obtained for the same sample of 11 Calán/Tololo events but ignoring the peak luminosity–decline rate relation [Eqs. (9) and (10)]. *Hence, we conclude that in using SN 1972E to determine the zero point of the Hubble law for SNe Ia, the effect of neglecting the peak luminosity–decline rate relation is to underestimate H_0 by ~15%.*

The case of SN 1937C, the other SN Ia with a Cepheid distance, is presently controversial. Based on Leibundgut's compilation of photographic photometry from various sources for this SN, Saha *et al.* (1994a) estimate $B_{MAX} = 8.83 \pm 0.11$ and $V_{MAX} = 8.64 \pm 0.10$ to infer a value of $H_0 = 52 \pm 9$ km s^{-1} Mpc^{-1}. However, in a recent work, Pierce *et al.* (1993, 1994) have scanned with a PDS microdensitometer the original plates obtained by Zwicky and find that the maximum light magnitudes of SN 1937C in B and V were ~0.2 and ~0.4 mag, respectively, fainter than those assumed by Saha *et al.* (1994a), leading to a significant increase of the Hubble constant. In addition, Pierce's *et al.* results lead to a change in the shape of the light curve, converting 1937C from a typical SN Ia into a slow decliner. In the frame of the peak luminosity–decline rate relation, the corrected B and V magnitudes of SN 1937C become ~0.3 and ~0.5 mag fainter, respectively, than the Saha *et al.* values. Given this present conflict in the estimates of the peak magnitudes of SN 1937C, we have chosen to restrict the current discussion solely to SN 1972E. Clearly, the determination of the zero point of SNe Ia luminosities is still at an early stage—future attempts to measure Cepheid distances should concentrate on well observed SNe Ia for which accurate decline rates can be determined.

Studies of the historical data have provided tentative evidence that SNe Ia in early-type (E,S0,Sa) galaxies have Si II expansion velocities which are systematically lower than those observed in late-type spiral and irregular galaxies (Filippenko 1989; Branch & van den Bergh 1993), suggesting that the progenitors of SNe Ia in late-type galaxies may be drawn from a younger population. Although the number of SNe included in the present study is relatively small, we find that galaxies having a younger stellar population (bluer color) appear to host the intrinsically brightest SNe Ia. This observation, which suggests that luminous SNe Ia may be associated with more massive progenitors, is consistent with the assertion by Della Valle & Livio (1994) that a significant fraction of the SNe Ia discovered in spirals appear superposed on the arms of the parent galaxies. The implications for cosmological studies are at least two-fold. First of all, the use of Pop I objects such as Cepheids to calibrate the zero point of the SNe Ia Hubble diagram could bias the results toward luminous SNe Ia. This may account for the fact that both SNe Ia with Cepheid distances, 1937C and 1972E, appear to have been luminous, slow-declining events. Likewise, the use of SNe Ia to determine q_0 is clearly susceptible to a systematic bias since, with increasingly larger look-back times, one will be sampling galaxies at correspondingly earlier stages in their star formation history. In principle, both of these biases can be overcome through further verification and calibration of the peak luminosity–decline rate relation. Nevertheless, the measurement of q_0 becomes a considerable observational challenge since accurate measurements of the decline rates for SNe Ia at redshifts of 0.3–0.5 will be required.

5. CONCLUSIONS

(1) We have constructed the Hubble diagrams in B and V for a group of 13 well observed SNe Ia spread over an unprecedented range in redshifts. Clear evidence is found for a distance-dependent scatter which we argue is due to an intrinsic dispersion in absolute magnitude of ~0.8 mag in M_B and ~0.5 mag in M_V. If the progenitors of low luminosity events like SN 1991bg are actually helium stars, as recently suggested by Woosley *et al.* (1994), then the intrinsic dispersion in M_B and M_V for SNe Ia with white dwarf progenitors is probably more like 0.3–0.5 mag.

(2) We have confirmed in general terms the finding by Phillips (1993) that absolute B and V magnitudes at maximum light of SNe Ia are correlated with the initial decline rate of the B light curve. This effect appears to be well defined over the range of decline rates $0.8 < \Delta m_{15}(B) < 1.5$. At faster decline rates, the dispersion may increase, but further observations of such fast events are required to verify this.

(3) Our analysis shows that galaxies having a younger stellar population (bluer color) appear to host the intrinsically brightest SNe Ia. This finding suggests that luminous SNe may be associated with more massive progenitors, posing potential problems to the determination of both H_0 and q_0.

(4) Analysis of the photometry of SN 1972E in NGC 5253 indicates that this object was a slow-declining event. The recently measured Cepheid distance to NGC 5253 implies a Hubble constant in the range $H_0 = 62$–67 km s^{-1} Mpc^{-1} if the peak luminosity–decline rate relation for SNe Ia is taken into account. The effect of ignoring the dependence of the peak luminosity on the initial decline rate leads, in this case, to an underestimate of H_0 by ~15%.

We plan to test these conclusions as soon as the light curves for the complete Calán/Tololo sample of ~25–30 SNe Ia are fully reduced. In addition, we shall extend our study of the Hubble diagram to the R and I bands which have not been treated to date due to the lack of published data. In a recent paper, Suntzeff (1994) has shown that there is quite a variety among the light curve shapes of SNe Ia in these bands which will complicate the task of deriving peak magnitudes for those SNe observed after maximum light. On the other hand, the evidence from the Phillips (1993) sample of nearby SNe is that the intrinsic dispersion in the absolute magnitudes at maximum light of SNe Ia is substantially smaller in the I band than in either B or V. This fact, combined with the decreased effect of dust extinction, suggests that the R and I bands may offer greater promise yet for the use of SNe Ia as cosmological standard candles.

REFERENCES

Branch, D., & van den Bergh, S. 1993, AJ, 105, 2231

Burstein, D., & Heiles, C. 1982, AJ, 87, 1165

Capellaro, E., Turatto, M., Benetti, S., Tsvetkov, D. Y., Bartunov, O. S., & Makarova, I. N. 1993, A&A, 273, 383

Della Valle, M., & Livio, M. 1994, ApJ, 423, L31

de Vaucouleurs, G., de Vaucouleurs, A., Corwin, H. G., Buta, R. J., Paturel, G., & Fouqué, P. 1991, Third Reference Catalogue of Bright Galaxies (Springer, Berlin)

Dressler, A., Faber, S. M., Burstein, D., Davies, R. L., Lynden-Bell, D., Terlevich, R. J., & Wegner, G. 1987, ApJ, 313, L37

Filippenko, A. V. 1989, PASP, 101, 588

Filippenko, A. V., et al. 1992, AJ, 104, 1543

Hamuy, M., et al. 1993a, AJ, 106, 2392 (Paper I)

Hamuy, M., Phillips, M. M., Wells, L. A., & Maza, J. 1993b, PASP, 105, 787

Hamuy, M., et al. 1994, AJ (in press) (Paper III)

Hough, J. H., Bailey, J. A., Rouse, M. F., & Whittet, D. C. B. 1987, MNRAS, 227, 1P

Jacoby, G. H., et al. 1992, PASP, 104, 599

Kowal, C. T. 1968, AJ, 73, 1021

Leibundgut, B. 1988, Ph.D. thesis, University of Basel

Leibundgut, B. 1990, in Supernovae, edited by S. E. Woosley (Springer, Berlin), p. 751

Leibundgut, B., Tammann, G. A., Cadonau, R., & Cerrito, D. 1991, A&AS, 89, 537

Leibundgut, B., et al. 1993, AJ, 105, 301

Maza, J., Hamuy, M., Phillips, M. M., Suntzeff, N. B., & Avilés, R. 1994, ApJ, 424, L107 (Paper II)

Phillips, M. M., et al. 1987, PASP, 99, 592

Phillips, M. M., Wells, L. A., Suntzeff, N. B., Hamuy, M., Leibundgut, B., Kirshner, R. P., & Foltz, C. B. 1992, AJ, 103, 1632

Phillips, M. M. 1993, ApJ, 413, L105

Phillips, M. M., & Eggen, O. J. 1994 (in preparation)

Pierce, M. J., Jacoby, G. H., & Carder, E. 1993, BAAS, 25, 1404

Pierce, M., et al. 1994 (in preparation)

Pskovskii, Y. P. 1967, SvA, 11, 63

Ruiz-Lapuente, P., et al. 1993, Nature, 365, 728

Saha, A., Labhardt, L., Schwengeler, H., Macchetto, F. D., Panagia, N., Sandage, A., & Tammann, G. A. 1994a, ApJ, 425, 14

Saha, A., Sandage, A., Labhardt, L., Schwengeler, H., Tammann, G. A., Panagia, N., & Macchetto, F. D. 1994b, ApJ (submitted)

Sandage, A. 1961, The Hubble Atlas of Galaxies (Mount Wilson and Palomar Observatories, Carnegie Institution of Washington, and California Institute of Technology)

Sandage, A., Saha, A., Tammann, G. A., Panagia, N., & Macchetto, D. 1992, ApJ, 401, L7

Sandage, A., & Tammann, G. A. 1993, ApJ, 415, 1

Sandage, A., Saha, A., Tammann, G. A., Labhardt, L., Schwengeler, H., Panagia, N., & Macchetto, F. D. 1994, ApJ, 423, L13

Shaw, R. L. 1979, A&A, 76, 188

Suntzeff, N. B. 1994, in Supernovae and Supernovae Remnants, IAU Colloquium No. 145, edited by R. McCray (Cambridge University Press, Cambridge) (in press)

Tammann, G. A., & Leibundgut, B. 1990, A&A, 236, 9

Vaughan, T. E., Branch, D., Miller, D. L., & Perlmutter, S. 1994, preprint

van den Bergh, S., & Pazder, J. 1992, ApJ, 390, 34

Woosley, S. E., & Weaver, T. A. 1994, ApJ, 423, 371

Woosley, S. E., Larger, N., & Weaver, T. A. 1994, ApJ (submitted)